Chapter 2

Advanced Fabrication and Properties of Aligned Carbon Nanotube Composites: Experiments and Modeling

Hai M. Duong, Feng Gong, Peng Liu and Thang Q. Tran

Additional information is available at the end of the chapter

http://dx.doi.org/10.5772/62510

Abstract

Aligned carbon nanotube (CNT) composites have attracted a lot of interest due to their superb mechanical and physical properties. This article presents a brief overview of the synthesis approaches of aligned CNT composites. The three major methods for fabricating aligned CNT fibers are first reviewed, including wet-spinning, dry-spinning and floating catalysts. The obtained CNT fibers, however, have limited mechanical and physical properties due to their porous structure and poor CNT alignment within the fibers. Appropriate treatments are required to densify the fibers to enhance their properties. The main approaches for the densification of CNT fibers are then discussed. To further enhance load transfer within CNT fibers, polymer infiltration is always used. Typical studies on polymer infiltration of CNT fibers are reviewed, and the properties of the obtained composites indicate the superiority of this composite fabrication method over the conventional dispersion method. Since aligned CNT composites are usually obtained in structures of long fiber or thin film, it is difficult to measure the thermal conductivity of these composites. An off-lattice Monte Carlo model is developed to accurately predict the thermal conductivity of aligned CNT composites.

Keywords: Aligned CNT composite, CNT fiber, fiber densification, polymer infiltration, Monte Carlo model

1. Introduction

Both single-walled nanotubes (SWNTs) and multi-walled nanotubes (MWNTs), which possess remarkable multifunctional properties such as high Young's modulus of 1 TPa [1], ultrahigh thermal conductivity of 2000–3500 W/mK [2,3], and outstanding electrical conductivity of 3×10^4

S/cm [4], have attracted much attention over the past decades [5]. Carbon nanotubes (CNTs) have been considered promising effective additives for developing high-performance composites. Currently, in the widely-used approaches for fabrication of CNT-based composites, CNTs are randomly dispersed into the matrix. This approach, however, typically results in low volume fraction, poor dispersion and random orientation of CNTs in matrices, inducing very limited enhancements and much lower properties than expected. To overcome these limitations, various CNT Structures such as buckypapers [6], CNT arrays [7–9], and CNT yarns [10] have been developed to pre-arrange the CNTs prior to fabricating composites.

Among those CNT post-treatments, assembling CNTs into CNT fibers has attracted tremendous attention. In general, there are three major methods for production of CNT fibers: (1) wet-spinning from CNT/acid or polymer solutions [11–13]; (2) dry-spinning from vertically aligned CNT arrays [10,14–17]; and (3) direct-assembling from CNT aerogels formed in chemical vapor deposition (CVD) [5,18–24]. The first method is also known as the wet-spinning method, while the others are known as dry-spinning methods.

The obtained CNT fibers commonly possess satisfactory mechanical and electrical properties [5], and even higher strength and better flexibility than commercial carbon fibers and polymer fibers [25]. In order to further improve their properties (mechanical strength in particular), polymer infiltration is usually performed on the CNT fibers to obtain CNT fiber/polymer composites. The polymer can greatly enhance the inter-tube load transfer, inducing high mechanical strength of the composites.

2. Methods for assembling CNTs into CNT fibers

2.1. Spinning from CNT Solution

In 2000, Vigolo et al. [11] first fabricated CNT ribbons and fibers via the coagulation spinning approach that was widely used to synthesize polymer fibers. **Figure 1**(**a**) shows the schematic of the experimental setup used to make nanotube ribbons. In this method, SWNTs are homogeneously dispersed in a solution of sodium dodecyl sulfate (SDS), which helps prevent CNTs from agglomeration. The CNT dispersion is then injected into the co-flowing stream of a polymer solution that contains 5.0 wt.% of polyvinylalcohol (PVA) to form CNT ribbons, as shown in **Figure 1**(**b**). **Figure 1**(**e**) shows a typical SEM image of the as-obtained CNT ribbon, revealing a preferential orientation of the nanotubes along the ribbon's main axis. After the ribbons are washed and dried, most of the surfactants and polymers are removed. The ribbons are collapsed into fibers due to capillary force, as shown in **Figure 1**(**c**). These fibers are more flexible than traditional carbon fibers, as shown in **Figure 1**(**d**). The diameter of CNT fibers varies from 10 to 100 μm depending on fabrication conditions. The tensile strength, modulus and electrical conductivity of the obtained fibers are 300 MPa, 40 GPa and 10 S/cm, respectively.

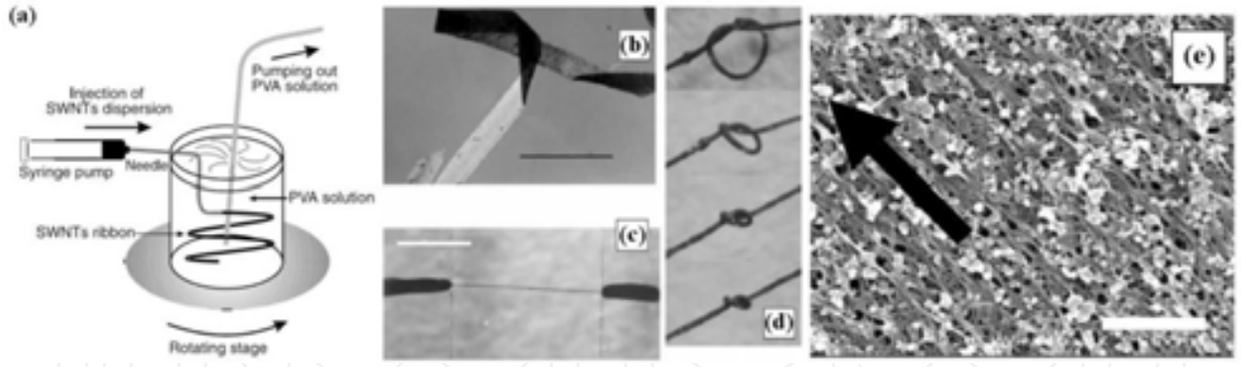

Figure 1. (a) Schematic of the experimental setup used to make nanotube ribbons. (b–d) Optical micrographs of nanotube ribbons and fibers. (b) A single folded ribbon between horizontal and vertical crossed polarizers (scale bar = 1.5 mm); (c) A freestanding nanotube fiber between two glass substrates (scale bar = 1 mm); and (d) Tying knots reveals the high flexibility and resistance to torsion of the nanotube microfibers. (e) Scanning electron micrograph shows SWNT bundles are preferentially oriented along the main axis of the ribbon (scale bar = 667 nm) [11].

Vigolo's technique is remarkable for further studies on fabricating continuous CNT fibers on a large scale, although this technique has some disadvantages. For example, the drawing of these as-spun gel fibers is slow (~1 cm/min), and the solid fibers are short (~10 cm) [26]. In addition, the fibers' mechanical properties are low compared with those of component individual nanotubes. Moreover, mechanical performance is improved, mostly because PVA chains in a CNT fiber enhance load transfer efficiency between CNTs. However, the existence of the non-conductive PVA leads to lower electrical and thermal conductivity of the obtained CNT fibers than pure CNT sheets [27]. Thus, fibers composed solely of CNTs are desirable. In 2004, Ericson et al. [12] developed a method to fabricate well-aligned macroscopic fibers composed solely of SWNTs. In this method, purified SWNTs are dispersed in 102% sulfuric acid, which charges SWNTs and promotes their ordering into an aligned phase of individual mobile SWNTs surrounded by acid anions. This ordered dispersion is extruded into continuous lengths of macroscopic neat SWNT fibers. The obtained fibers possess a Young's modulus of 120 ±10 GPa and a tensile strength of 116 ±10 MPa. Because these pure CNT fibers do not contain polymers, they demonstrate better electrical and thermal properties than fibers containing polymers, with an electrical conductivity of 500 S/cm and thermal conductivity of ~21 W/m K. In another method proposed by Behabtu et al. [13], high-quality CNTs are dissolved in chlorosulfonic acid and extruded into a coagulant (acetone or water) to remove the acid. The forming filament is further stretched and tensioned to ensure high CNT alignment in the structure. The resulting fibers possess a Young's modulus of 120 ± 50 GPa and strength of 1.0 ± 0.2 GPa. The tensile strength shows a tenfold improvement over wet-spun fibers fabricated using the method developed by Ericson et al. [12]. At the same time, they display outstanding electrical conductivity (~29000 ± 3000 S/cm) and thermal conductivity (~380 ± 15 W/m K).

2.2. Spinning from vertically aligned CNT arrays

Just like drawing a thread from a silk cocoon, CNT fibers can be synthesized from a vertically aligned CNT array. In 2002, Jiang et al. [10] spun a 30-cm-long CNT fiber from a CNT array

(~100 μm in height). In 2004, Zhang et al. [14] modified this technique by introducing twist during spinning. In this method, the nanotube arrays (~30 μm in height) are grown on an iron catalyst–coated substrate by CVD. Afterward, yarns are drawn from the array and twisted with a variable-speed motor. **Figure 2**(**a**) and (**b**) clearly show the SEM images of the structures formed during the spinning process. The obtained fibers have a tensile strength of ~460 MPa, modulus of ~30 GPa and electrical conductivity of 300 S/cm.

Since then, many efforts have been made to optimize spinning processes and to improve the performance of CNT fibers. Spinning fibers from higher CNT arrays can effectively improve fiber performance. For example, Zhang et al. [15] reported the spinning of CNT fibers from relatively long CNT arrays (0.65 mm), which resulted in the strength and Young's modulus of the CNT fibers reaching 1.91 GPa and 330 GPa, respectively. Furthermore, Li et al. [16] spun CNT fibers from 1 mm CNT arrays. Their tensile strength reached up to 3.3 GPa, which is much higher than that of CNT fibers from the 0.65 mm array. In aiming to achieve the goal of providing a continuous process for the solid-state fabrication of CNT yarns from CNT forests, Lepro et al. [17] spun fibers from CNT forests grown on both sides of highly flexible stainless steel sheets, instead of the conventionally used silicon wafers, as shown in **Figure 2**(**c**), (**d**) and (**e**). They reported that the catalyst layer is shown to be re-usable, decreasing the need for catalyst renewal during a proposed continuous process.

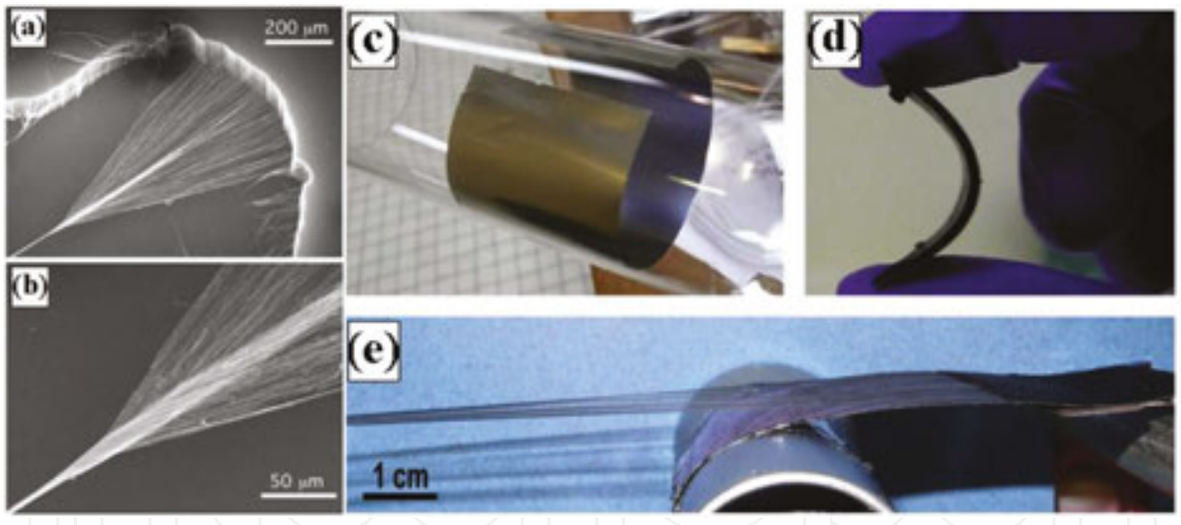

Figure 2. (a) and (b) SEM images of a carbon nanotube yarn in the process of being simultaneously drawn and twisted during spinning from a nanotube forest outside the SEM [14]; (c–e) Spinnable CNT forest grown on flexible stainless steel substrate [28].

Studies have found that not all CNT arrays can be spun into fibers, and the degree of spinnability of CNTs is closely related to the morphology of CNT arrays [29,30]. Several research groups have made efforts to study the mechanism of spinning fibers from CNT arrays. Kuznetsov et al. [28] developed a structural model for the drawing of sheets and fibers from CNT arrays. Huynh et al. [30] studied the roles of catalyst, substrate, temperature, gas flow rates, reaction time with acetylene, etc. to identify and understand the key parameters and

http://dx.doi.org/10.5772/62510

develop a robust, scalable process. More recently, Zhu et al. [31] pointed out that the entangled structures at the ends of CNT bundles are critical for the continuous drawing process. Further fundamental studies of this mechanism are critical for fabricating spinnable CNT arrays and improving the properties of CNT fibers.

2.3. Spinning from CNT aerogels

In both of the above-mentioned methods, individual CNTs are first produced in the form of CNT powders or arrays. In this method, fibers are achieved through the post-process of spinning. Unlike the in-direct methods, CNT fibers can be assembled directly in a CVD process in which individual CNTs are synthesized. In 2000, Zhu et al. [18] first reported the direct synthesis of 20cm long ordered SWNTs with a diameter of approximately 0.3mm using a floating catalyst CVD method in a vertical furnace. In 2004, Li et al. [19] reported a method for the direct spinning of long CNT fibers from aerogels formed during CVD. **Figure 3**(**a**) is a schematic of this direct spinning process. In this method, reaction precursors are mixed and introduced into a tube furnace operated at 1200°C. In a reducing hydrogen atmosphere, the

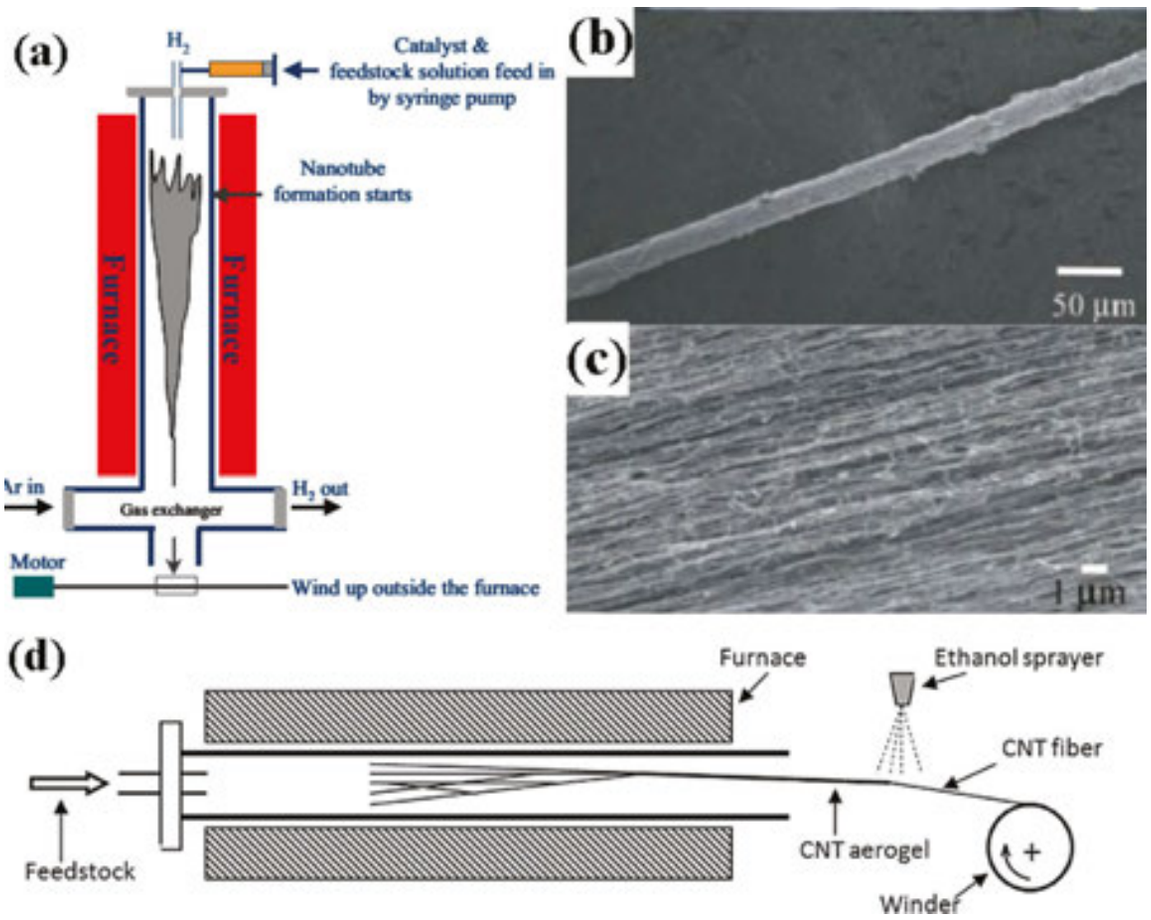

Figure 3. (a) Schematic diagram of the direct spinning process for CNT fibers [21]; (b) and (c)SEM micrographs of a fiber that consists of well-aligned MWNTs [19]; (d) Schematic diagram of the CNT fiber-spinning process using a horizontal furnace [24].

nanotubes form an aerogel in the hot zone of the furnace and are stretched into cylindrical hollow socks which are then pulled and collected continuously out of the furnace as fibers. **Figure 3**(**b**) and (**c**) show SEM images of the aligned CNT fibers after condensation by acetone vapor. CNT fibers, spun directly and continuously from aerogels, demonstrate both high strength (up to 357 GPa) and high stiffness (8.8 GPa), which are comparable to those of commercial fibers [20].

3. Methods for enhancing CNT alignment

The as-spun CNT fibers fabricated using the above methods usually have a porous structure, and the CNTs within the fibers have poor alignment [14,19,32]. Hence, the CNT fibers should be further densified to obtain a more closely-packed structure and better alignment of the CNTs. Since the van der Waals interaction strongly depends on the contact area between CNTs, much space and many pores between CNT bundles could lower the degree of this interaction. By applying the densification process, the densified CNT fibers can have reduced interspace between CNTs and an improved contact area, leading to an increased van der Waals interaction. As a result, these highly dense structures have a stronger van der Waals interaction between CNT bundles, hence improving fiber performance [32–34].

3.1. Enhancing CNT alignment for fibers spun from the wet-spinning technique

While classical composite fibers consist of CNTs embedded in a polymeric matrix, fibers fabricated by the wet-spinning technique consist of an interconnected network of polymers and CNTs. The spinning conditions, such as the flow velocity of the polymer solution and the injection rate of the CNT solution, has no measurable effect on the CNT orientation in the resulting fibers. However, when the fibers are immersed in an appropriate solvent or heated, the network of polymers and CNTs can be loosened and stretched, resulting in a significant improvement in CNT alignment. For example, Vigolo et al. [35] enhanced the CNT alignment of their SWNT/PVA fibers by re-wetting, swelling and re-drying the fibers vertically under a tensile load with a weight attached to the end of the fiber. The solvent used in the study was comprised of water, acetone and acetonitrile. Once re-wetted and swollen by the solvent, the fibers could be stretched up to 160% with significantly improved alignment, as shown in **Figure 4**. This indicates that the networks of CNTs and absorbed polymers form cross linked assemblies that can be elastically deformed. As a result, their strength and stiffness increased from 10 GPa and 125 MPa, to 40 GPa and 230 MPa, respectively, after the stretching.

Separately, Miaudet et al. [36] reported an increase in tensile strength of CNT/PVA fibers from 1.4 GPa to 1.8 GPa after the hot-stretched treatment. The reduction of PVA chain alignment from ±27° to as low as 4.3°, and the nanotube alignment to as low as 9°, suggested that better alignment of the CNT and PVA chains was the main reason for the improved mechanical performance of the hot-stretched fibers.

http://dx.doi.org/10.5772/62510

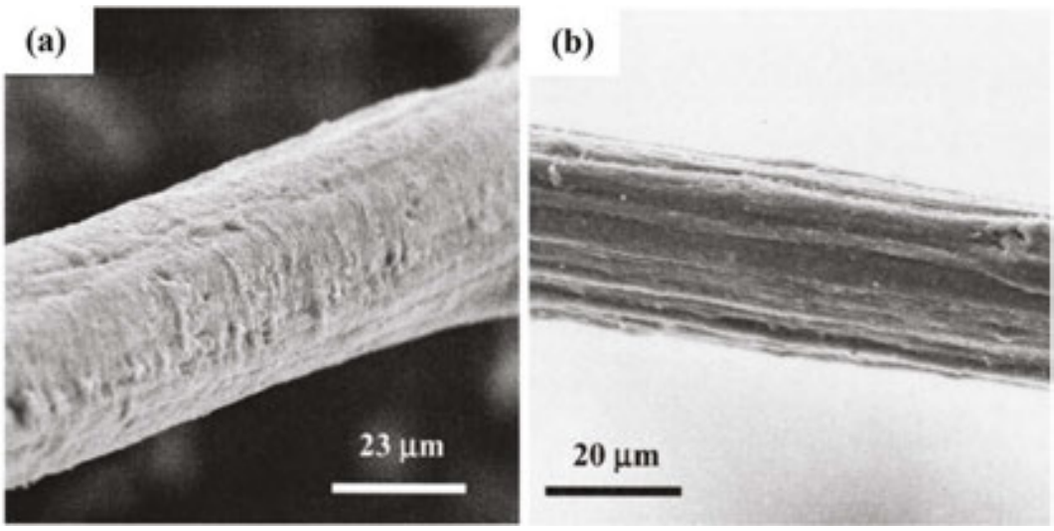

Figure 4. SEM images of an as-spun fiber (a), and (b) a stretched CNT fiber [35].

3.2. Enhancing CNT alignment for fibers spun from dry-spinning and floating catalyst techniques

CNT fibers spun from dry-spinning and floating catalyst techniques can be densified by applying a mechanical force in their lateral direction. The densification methods can be classified into two categories: indirect approaches (such as liquid densification, twisting [32], drawing through dies [37], or an aligning and tension system [38]); and direct approaches (such as rubbing/false twisting [39] and mechanical compression [40]).

3.2.1. Indirect approaches

3.2.1.1. Liquid densification

The alignment and mechanical performance of as-spun CNT fibers can be improved through liquid densification. In this method, a liquid such as acetone or ethanol is absorbed into the fibers and subsequently evaporated, resulting in a dense CNT structure. The fibers are densified due to the surface tension of the solvent and the fiber diameter is reduced accordingly. The densification process slightly improves nanotube alignment (**Figure 5**) and enhances load transfer between nanotubes, ensuring that most of them are fully load-bearing. Liu et al. [41] studied the mechanical properties of twisted fibers with and without acetone densification. The diameter of the yarn changed from 11.5 to 9.7 μm after shrinking. Although the maximum strain of the yarn remained unchanged (~2.3%), the Young's modulus (~56 GPa) of the shrunk fiber was slightly greater than before shrinking (~48 GPa). Liu et al. [41] also reported a change in diameter and maximum load of twisted fibers before and after shrinking. After acetone shrinking, the diameter reduction ranged from 15% to 24%, and the load increase ranged from 15 to 40%, indicating that tensile strength was enhanced. Among common solvents (water, ethanol and acetone) used to shrink CNT yarns, acetone showed the best shrinking effect.

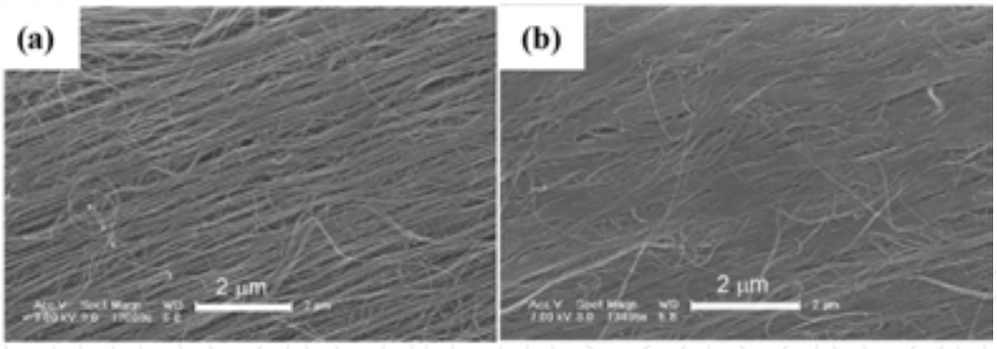

Figure 5. (a) SEM images of a twisted fiber before, and after shrinking (b) [41].

3.2.1.2. Twisting

The as-spun fiber is relatively loose with noticeable spaces between CNT bundles. Increasing the twist angle is an effective method for densifying CNT fibers. Since it brings CNTs into closer contact with each other, twisting improves the friction coefficient μ between CNTs, therefore contributing positively to fiber strength [15]. Zhang et al. [15] compared the tensile behaviors of twisted and untwisted CNT fibers spun from the same 650 mm height array. After twisting, the diameter of the fiber decreased from 4 to 3 μm (**Figure 6**), while tensile strength increased from 0.85 GPa to 1.9 GPa [15].

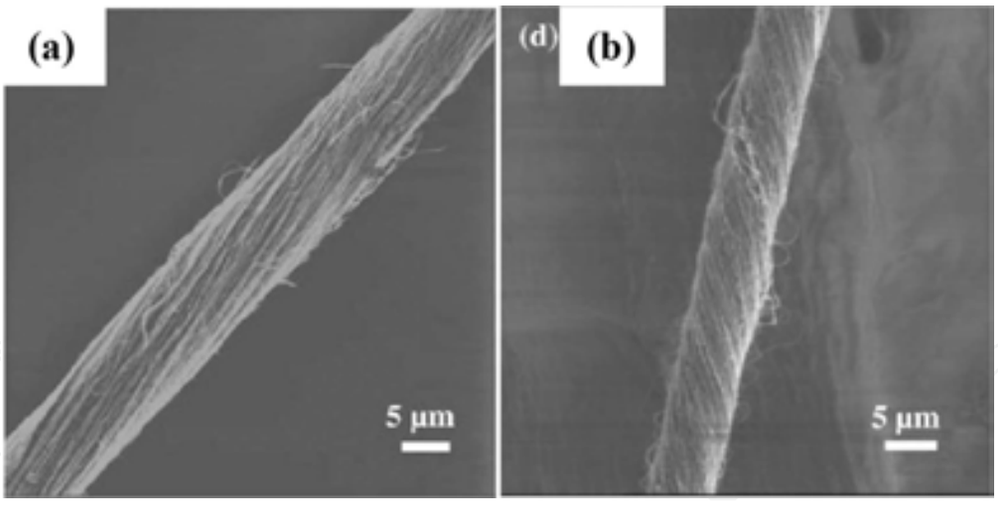

Figure 6. SEM images of as-spun CNT fiber (a), and the same fiber after post-spin twisting (b) [15].

3.2.1.3. Drawing through dies

The as-spun CNT fibers can be densified by being drawn through dies of different diameters. The average measured fiber diameter was determined by die size. Sugano et al. [37] densified CNT fibers spun from CNT arrays by drawing them through densifying dies with different diameters (d = 30, 35, 55, 75 μm) (**Figure 7**(**a**)). The fibers were deformed elastically after

http://dx.doi.org/10.5772/62510

drawing CNTs through the die, and their density increased with decreasing die diameter. As CNT fibers are held together by van der Waals forces between MWNTs, these forces increased due to higher apparent density with decreasing distance between MWNTs, as shown in **Figure 7**(**b**). As a result, their strength was significantly enhanced after treatment.

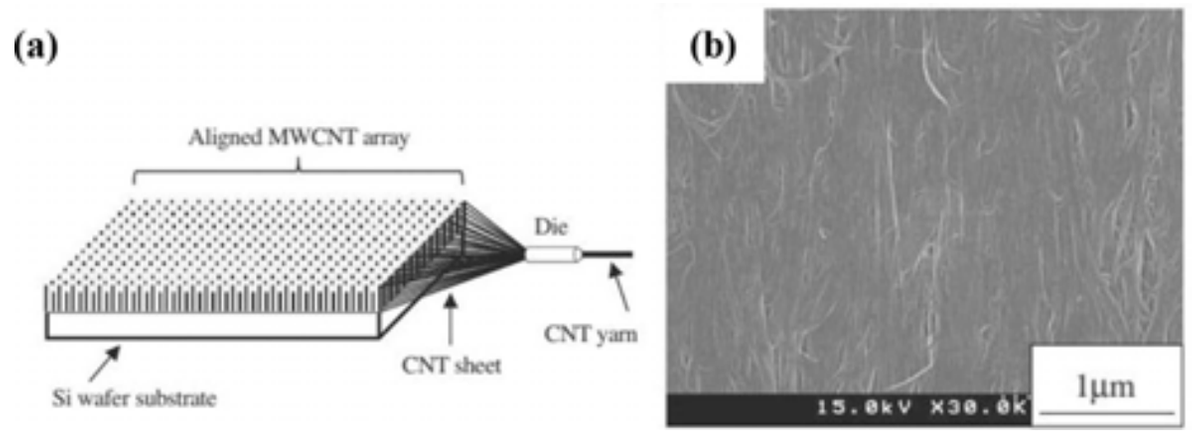

Figure 7. (a) Schematic view of untwisted CNT yarn in the process of being drawn from the aligned MWNT array and past the sheet through a die; (b) SEM image of surface morphologies of the resulting CNT fiber.

3.2.1.4. Aligning and tension system

The aligning and tension system is one of the most effective methods of enhancing CNT alignment and performance of CNT fibers. Tran et al. [38] first modified the traditional dry-spinning process to improve CNT alignment of their CNT fibers (**Figure 8**(**a**)). In this modified system, a capstan effect rod system (CERS) is added to a dry-spinning system to regulate tension and torque to the fibers. As the fibers pass through a CERS, the increased tension extends and aligns the bundles (**Figure 8**(**b**) and **8**(**c**)). This process has two effects: (i) aligning CNTs in the fibers during the initial tensioning; and (ii) condensing the CNT bundles. The first effect increases contact length between bundles, and the second effect reduces the distance between CNTs. The significant increase in fiber strength from 0.45 to 1.2 GPa after the treatment is due to better alignment of the fiber bundles and higher fiber compaction.

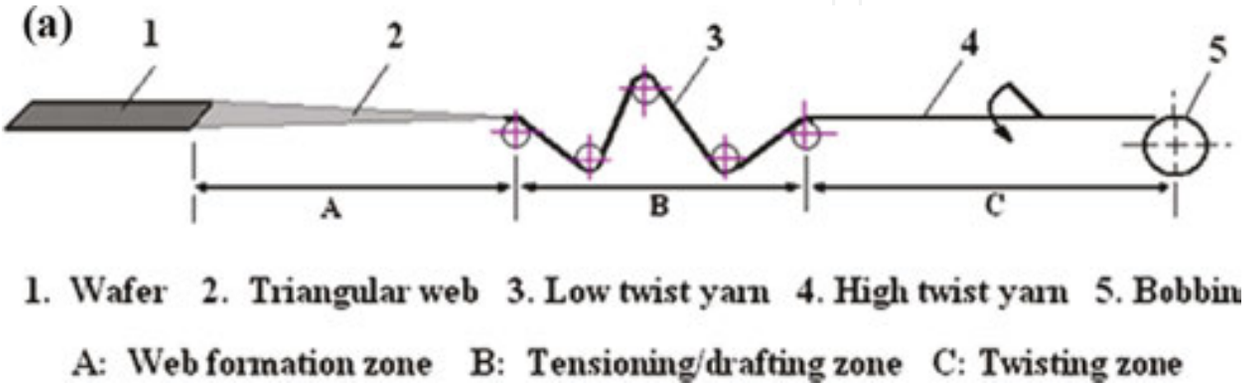

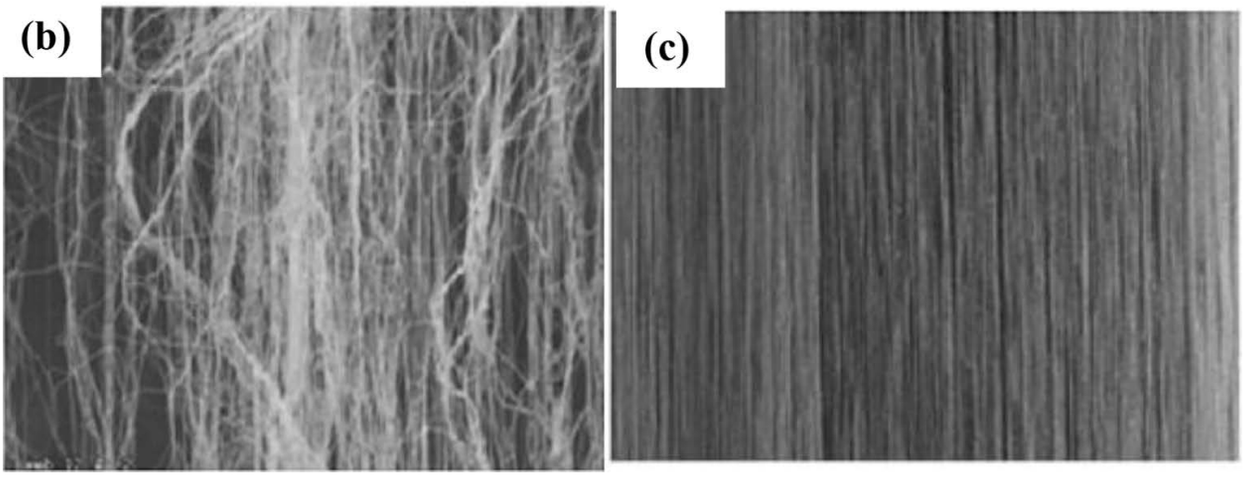

Figure 8. (a) The schematic of modified CNT yarn spinning; (b) SEM images of surface morphologies of CNT fiber spun from traditional process; and modified process (c) [38].

Generally, the drawback of the indirect approaches is their low densifying forces. The liquid densification method, for example, employs the surface tension of volatile solvents such as acetone or ethanol to densify the CNT fibers. Its densifying force is therefore limited by the low surface tension of the solvents used [32]. Similarly, the compressive force produced by drawing CNT fibers through a die results from the drawing forces and the die size used. These drawing forces are limited by fiber strength, while a significantly smaller die could damage the fiber structure, resulting in poor strength [37]. Therefore, CNT fibers cannot be adequately densified with these methods, and their performance remains unsatisfactory.

3.2.2. Direct approaches

Direct approaches are considered the best solution to overcome the above limitations. As the densifying forces are applied directly to CNT fibers, the forces can condense the fibers into a much denser structure [40].

3.2.2.1. Rubbing/false twisting

CNT fibers can be densified using several traditional textile twistless methods such as rubbing. Miao et al. [39] used a rubbing roller system (**Figure 9**(**a**)) to densify CNT web drawn from a vertically aligned CNT forest into a compact twistless yarn. As the system used a constant rate false twisting process, there is only a temporary twist on the incoming side of the yarn, and the yarn on the outgoing side (and thus the final yarn) will be twistless. As can be seen in **Figure 9**(**b**), the resulting yarn consists of a high packing density sheath with CNTs lying straight and parallel to the yarn axis, and a low density core with many microscopic voids. With an increased contact length between CNT bundles in the high packing density sheath, the mechanical performance of the core-sheath structured, twistless carbon nanotube yarns are significantly higher than that of their corresponding twist-densified yarns.

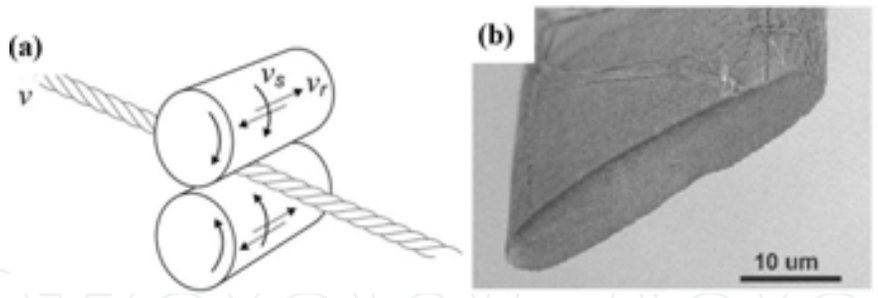

Figure 9. (a) The schematic of the core-sheath, twistless CNT yarn fabricated by a rubbing roller system; and (b) SEM image of the resulting yarn.

3.2.2.2. Mechanical compression

Wang et al. [40] reported that CNT fibers densified by the pressurized rolling system showed highly packed structures with a densification factor of up to 10 (**Figure 10**(**a**)). Moreover, the densified fibers can reach an impressive average strength of 4.34 GPa, which is the highest extrinsic CNT fiber strength reported to date [40]. In addition, Tran et al. [24] presented a modified densification method to produce a highly packed CNT structure. As shown in **Figure 10**(**b**), CNT fibers were sandwiched between two sheets of A4 paper and pressed by a stainless-steel spatula with an applied force of approximately 100 *N*, at 45° to the fiber axis. The spatula was subsequently slid across the A4 paper, along the fiber axis, to compress and mechanically densify the fibers into a ribbon shape while the compressive force was maintained. The CNT ribbon in this study also showed a densification factor of up to 10, while the strength and electrical conductivity of the densified fibers approached impressive values of 2.81 GPa and 12,000 S/cm, respectively. The study showed that the mechanical densification treatment may have increased the CNT bundle size and inter-CNT contact, and induced better alignment (**Figure 10**(**c**) and (**d**)), resulting in improved properties of the densified CNT fiber.

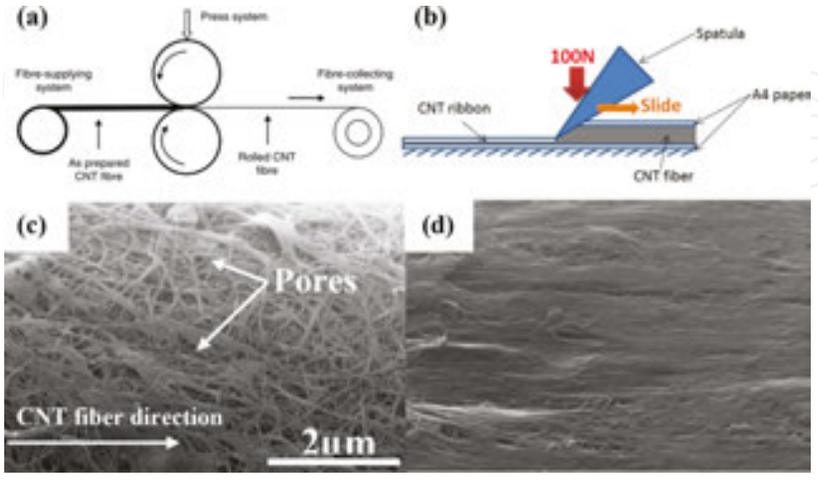

Figure 10. The schematic of mechanical densification methods using (a) pressurized rolling system, and (b) spatula; SEM images of the surface morphology of the (c) as-spun CNT fiber, and (d) densified CNT ribbons [24].

4. Mechanical and physical properties of aligned CNT polymer composites

The outstanding physical and mechanical properties of aligned CNT assemblies make them promising for the research and development of high-performance composites. The final properties of the composites are affected by many factors, such as, morphology of individual nanotubes and impregnating method.

4.1. Impregnating method

Pure CNT assemblies including fibers and films have an ineffective load transfer between CNTs as the CNTs interact with each other via weak van der Waals forces. Among all methods used to enhance load transfer between CNTs, polymer impregnation is one of the most effective treatments in enhancing the mechanical properties of CNT assemblies. This reinforcement mainly stems from the enhanced inter-tube load transfer and the crystallinity of the impregnated polymer. Several impregnating methods are used to fabricate aligned CNT polymer composites.

4.1.1. Dip coating/soaking

Dip coating or soaking is widely used to impregnate polymer into CNT assemblies. In this method, CNT assembles are immerged into polymer solution for sufficient infiltration and then taken out for curing. Liu et al. [32] reports the mechanical properties of PVA impregnated fibers spun from CNT arrays. **Figure 11** shows the schematic of the CNT/polymer fiber manufacturing process and compares the tensile properties of a CNT/PVA fiber with two types of pure CNT fibers. As can be seen, the CNT/PVA composite fiber with 19 wt.% PVA possesses a tensile strength of 1.95 GPa. This result is 255% higher than that of simply twisting the CNT fiber and 103% higher than that of a CNT fiber subjected to twisting and shrinking by acetone. The greater strength of the CNT/PVA fiber stems from the decrease in fiber diameter due to the high wettability between dimethyl sulfoxide (DMSO) and CNTs, and the increase in tensile load due to improved load transfer efficiency between CNTs after PVA impregnation (**Figure 11**(**b**)).

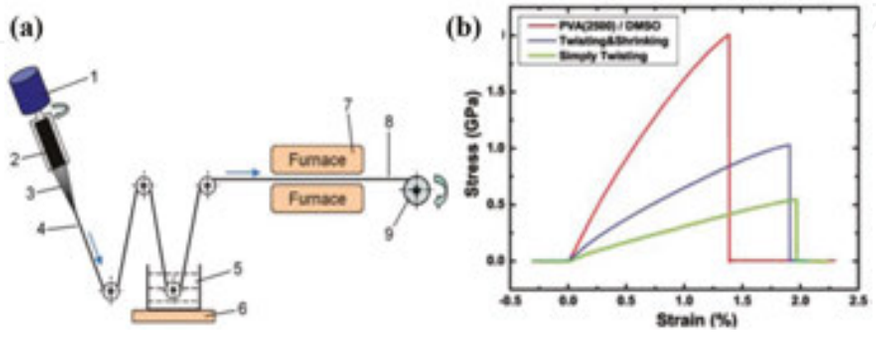

Figure 11. (a) Schematic of the CNT/polymer fiber manufacturing process; and (b) stress-strain curves of a typical SWNT/PVA yarn and two types of pure SWNT yarns. [32]

Similarly, Tran et al. [24] reported an outstanding enhancement of the electrical and mechanical performances of MWNT fibers through the combined treatments of mechanical densification and epoxy infiltration. Compared to the mechanical performances of CNT fibers produced by different post-treatments, the combined post-treatments employed in their study showed better effects, with enhancement factors of more than 13.5 for tensile strength and 63 for stiffness. After the first mechanical treatment, their condensed CNT ribbons achieved a tensile strength much greater than that of the best CNT fibers spun with wet-spinning and array-spinning methods, as shown in **Figure 12**. When further combined with epoxy infiltration, the CNT/epoxy ribbons reached significantly greater strength (up to 5.2 GPa) and stiffness (up to 444 GPa), which are very comparable to those of commercial PAN carbon fibers as shown in **Figure 12**. Furthermore, while the strength of their CNT/epoxy ribbons was comparable to that of the best double-walled CNT (DWNT) ribbons produced by the floating-catalyst method [40], their stiffness was much higher. The results suggest that by using a polymer infiltration treatment, the performance of MWNT fibers with low electrical and mechanical properties could achieve the performance of many other high-strength fibers.

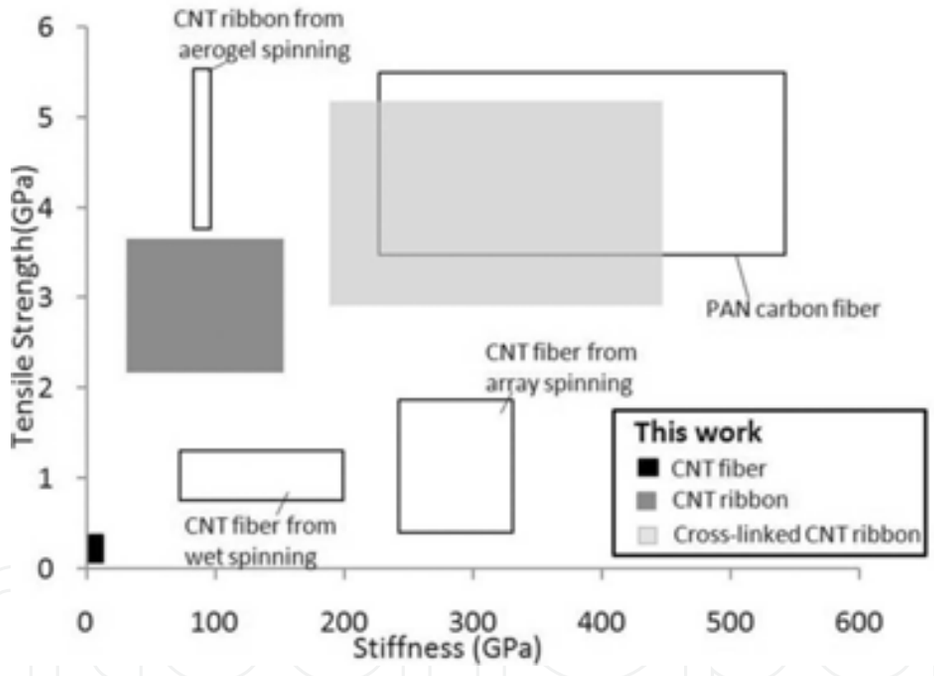

Figure 12. Comparisons of mechanical properties of the best CNT fibers from array-spinning [15] and wet-spinning [13], ribbons from aerogel spinning, and PAN carbon fibers [40].

Liu et al. [23] fabricated CNT/polyimide aerogel (CNT/PIA) composite fibers by dip-coating the CNT fibers in a sol solution, and then drying them using the supercritical CO_2 drying process. In the CNT/PIA composite fibers, CNT fibers are tightly wrapped by porous polyimide aerogel, showing a core-shell structure. This core-shell structure resulted in the light weight, low density and high surface area of the composite fiber. Owing to the superior properties of the CNT fibers (stiffness of ~450 MPa, tensile strength of ~83 MPa and electrical conductivity of ~419 S/cm), the CNT/PIA composite fibers achieve significant enhancements

in mechanical and electrical properties (stiffness of ~68.1 MPa, strength of ~11.6 MPa and electrical conductivity of ~418 S/cm), compared with the pure PIA and other CNT/PIA composite [42–46]. It was also found that the mechanical and electrical properties of CNT/PIA composite fibers decline with an increase in the diameter of CNT fibers.

4.1.2. Resin transfer molding

Resin transfer molding (RTM) is a very common and cost-effective method to fabricate composites in industries, in which the liquid resins are first injected to the preforms and then cured to be solid. Given its capability of making composites with large sizes and complex shapes, RTM is expected to be appropriate for preparing CNT/epoxy composites in large scale. Liu et al. [5] developed aligned CNT/epoxy composite films by combining layer-by-layer and vacuum-assisted RTM (VA-RTM) method using direct chemical vapor deposition (CVD)-spun CNT plies. The CNTs in the plies are well-condensed during the VA-RTM process (**Figure 13**(**a**)), leading to much higher mass fractions of CNTs (up to 24.4 wt.%) compared with those obtained from the conventional dispersion methods. Due to good alignment of the condensed CNTs in the plies, the CNT/epoxy composite with 24.4 wt.% CNTs achieves ~5 and ~10 times enhancements in their Young's modulus and strength, respectively. A high tensile toughness of up to 6.39 × 10^3 kJ/m^3 was also obtained in the composite films, making them promising candidates for protective materials, as shown in **Figure 13**(**b**). The electrical conductivity of the aligned CNT/epoxy composites reaches as high as 252.8 S/cm for the composite with 24.4 wt.% CNTs, which is ~20 times greater than that of the CNT/epoxy composites obtained using dispersion methods [47–49].

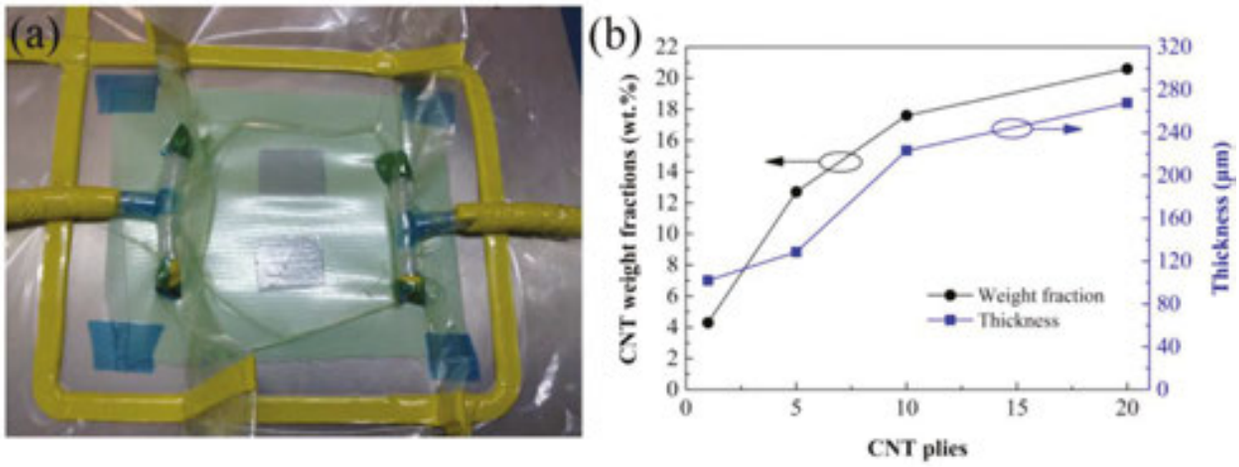

Figure 13. (a) Experimental set-up of the RTM process for preparing CNT/epoxy films; and (b) The CNT weight fractions and the thickness of CNT/epoxy composite films as a function of CNT plies. [5].

4.1.3. Spray winding and layer-by-layer deposition

The aforementioned methods are mostly regarded as off-line methods in which highly packed CNT assembles are used as preforms. Because the preforms are already tightly packed,

http://dx.doi.org/10.5772/62510

however, these methods often have the problem of the uniformity of infiltration. As a result, the un-infiltrated part may become defects and limit the overall performance of the composites [50]. In order to control the uniformity of infiltration and avoid over-infiltration, Liu et al. [50, 51] developed a one-step approach of "spray winding" to fabricate high-performance CNT composites. In this on-line infiltration method, CNT sheets, drawn out from CNT arrays, were continuously collected (wound) onto a rotating mandrel under the spray of a polymer solution, as shown in **Figure 14**(**a**). The spray-wound CNT/PVA composite films, the CNT fraction is tunable, and could be as high as 65 wt.% to reach the best mechanical properties. The best film had the tensile strength, stiffness and toughness up to 1.8 GPa, 45 GPa, and 100 J/g, respectively, much better than the fibers made by the same CNT and PVA and many other CNT/polymer composites. The high performance can be attributed to the long CNTs, highly-aligned tube morphology, and good interfacial bonding between CNT and PVA, which were obtained simultaneously. In order to control the exact layers of the composite films in large scale, Zhang et al. [52] reported a "layer-by-layer (LBL) deposition" method to produce CNT polymer composites, as shown in **Figure 12**(**b**). This on-line deposition method allowed PVA to infiltrate into the CNT film efficiently, resulting in a remarkable improvement in the mechanical property of CNT/PVA composite. The composite film possessed a tensile strength of 1.7 GPa, which is almost one order of magnitude and 20 times higher than those of the pure CNT and PVA films, respectively.

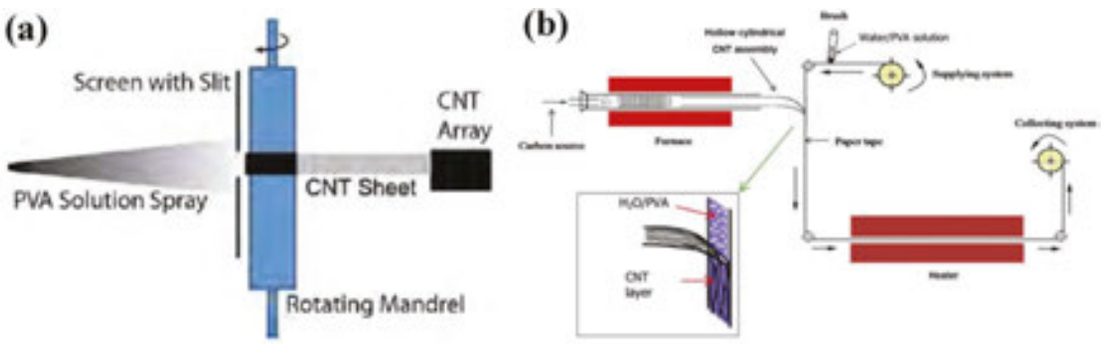

Figure 14. (a) Schematic view of spray winding [50]; and (b) Schematic illustration of the LBL deposition process [52].

4.2. Effect of CNT morphology

Individual nanotube morphologies, such as length and alignment, have great influence on mechanical and physical properties of CNT polymer composites. Wang et al. [53] reported an ultrastrong and stiff CNT/composite using a stretch-winding process. The unstretched composites exhibited strength of 2.0 GPa, Young's modulus of 130 GPa and electrical conductivity of 820 S/cm. After stretching the strength, Young's modulus and electrical conductivity were increased to as high as 3.8GPa, 293 GPa and 1230 S/cm, respectively. These remarkable improvements can be ascribed to the enhancement of CNT alignment and decreasing of waviness. The alignment of the CNTs was characterized by polarized Raman. Specifically, the shift of the intensity ratio (IG∥/IG⊥) of G band peaks was measured. Following the stretch-

winding process, the intensity ratio for the 12%-stretched sheet is increased to 7.6 from 1.6, indicating that alignment of the CNTs in the nanocomposites was significantly improve via the stretching process. Therefore, the improved CNT alignment is correlated with the observed improvements in mechanical and electrical properties of the composites.

Park et al. [54] studied the effects of nanotube length and alignment on thermal conductivity of MWNT/epoxy composites. It was found that the long-MWCNT composites exhibited higher thermal conductivity than the short-MWCNT composites with the same weight percentages. At room temperature, 10 wt.% short-MWCNT/epoxy composite showed thermal conductivity of 0.35 W/mK, while the long-MWCNT composites showed 2.6 W/mK even at lower concentration of 6.38 wt.%. To improve the in-plane thermal conductivity, CNT sheets (60 wt.%) were stretched mechanically. The thermal conductivity increased up to 83 W/mK (25% stretched) and 103 W/mK (40% stretched) along the alignment direction compared to 55 W/mK of the random sample.

5. Mesoscopic modeling of thermal conduction in aligned CNT composites

Due to the unique morphology of aligned CNT composites, it is difficult to directly measure their thermal conductivity, especially for composites in thin film and long fiber structures. Proper computational modeling is required to accurately predict the thermal conductivity of aligned CNT composites. The widely-used effective medium theories (EMTs) can well predict the thermal conductivity of CNT composites obtained using dispersion methods. However, the EMTs generally fail to predict the thermal conductivity of aligned CNT composites, since they cannot take into account the complex morphology of CNTs and the thermal boundary resistances (TBRs) at both CNT-CNT and CNT-matrix interfaces [55]. The TBRs are the resistances to the heat flow at interfaces, which have been regarded as the bottleneck of thermal conduction in CNT composites [56].

5.1. Thermal conduction model for two-phase aligned CNT composites

In order to accurately predict the thermal conductivity of aligned CNT composites, Duong et al. [57] developed an off-lattice Monte Carlo (MC) approach by quantifying thermal energy through a large quantity of random thermal walkers. Thermal walkers have a random Brownian motion in the polymer matrix, which is described by the position changes of thermal walkers in each direction. The position changes take values from a normal distribution with a zero mean and a standard deviation, as expressed as below:

$$\sigma = \sqrt{2D_{\mathrm{m}}\Delta t} \tag{1}$$

where D_{m} is the thermal diffusivity of polymer matrices, and Δt is the time increment of the simulation [58]. When a walker jumps to the CNT-polymer matrix interface, it may jump into the CNT with a probability $f_{\mathrm{m\text{-}CNT}}$, or remain within the polymer matrix with a probability (1-

$f_{\text{m-CNT}}$). The probability is a function of the TBR between polymer and CNT, $R_{\text{m-CNT}}$, obtained using the acoustic mismatch theory (AMT) [59]:

$$f_{\text{m}-\text{CNT}} = 4 / (\rho C_{\text{p}} v R_{\text{m-CNT}}) \tag{2}$$

where ρ is the density of polymer, C_{p} is the specific heat of polymer, and v is the sound velocity in the polymer matrix. Due to the ballistic phonon transport and ultrahigh thermal conductivity in the CNT [60], thermal walkers are assumed to travel at an infinite speed inside the SWNT [61]. The walker is allowed to exit from a CNT to the matrix by using another probability $f_{\text{CNT-m}}$, which is related to $f_{\text{m-CNT}}$ in a way that satisfies the second thermodynamic theorem [62, 63]:

$$V_{\text{CNT}} f_{\text{CNT}-\text{m}} = C_{f-\text{CNT}} \sigma_{\text{m}} A_{\text{CNT}} f_{\text{m}-\text{CNT}} \tag{3}$$

wherein V_{CNT} and A_{CNT} are the volume and surface area of a CNT, and σ_{m} is the standard deviation of Brownian motion in the polymer matrix. $C_{f\text{-CNT}}$ is the thermal equilibrium factor at the polymer-CNT interface, which is dependent on the geometry of the CNTs, and the interfacial area between the CNT and the matrix.

By using the developed MC approach, Duong et al modeled SWNT-epoxy and SWNT-polymethyl methacrylate (PMMA) composites [64]. The thermal conductivity of SWNT-epoxy and SWNT-PMMA composites were accurately predicted. The effects of the SWNT orientation, weight fraction and TBRs on the thermal conductivity of composites were quantified. The quantitative findings showed that in SWNT-PMMA composites with 1.0wt.% of SWNT loading, aligned SWNTs achieved enhanced thermal conductivity 15 times higher than that of PMMA, whereas, the randomly dispersed SWNTs only resulted in thermal conductivity ~5 times higher than that of PMMA [64]. This indicated the superiority of aligned CNT composites.

Since CNTs are normally grown into forests or spun into fibers, the contacts between CNTs may play a significant role to modify the thermal conductivity of composites. Duong et al. then modified their model to study the effect of CNT-CNT contacts on the thermal conductivity of both SWNT-epoxy and MWNT-epoxy composites [65,66]. A representative volume element (RVE) was built based on the real CNT-epoxy composites, as shown in **Figure 15**. In MWNT-epoxy composites with 20 vol % of MWNT loading, aligned MWNTs without contacts achieved a thermal conductivity nearly 40 times higher than that of epoxy, while, aligned MWNTs with contacts induced a thermal conductivity only 20 times higher than that of epoxy. This indicated that CNT-CNT contacts in aligned CNTs may reduce the thermal conductivity of composites. The anisotropic thermal conductivity of aligned CNT composites was also quantified. In both SWNT-epoxy and MWNT-epoxy composites, the thermal conductivity parallel to the aligned CNTs was much higher than that perpendicular to the aligned CNTs. The SWNT-epoxy composites had more significantly anisotropic thermal conduction than MWNT-epoxy composites.

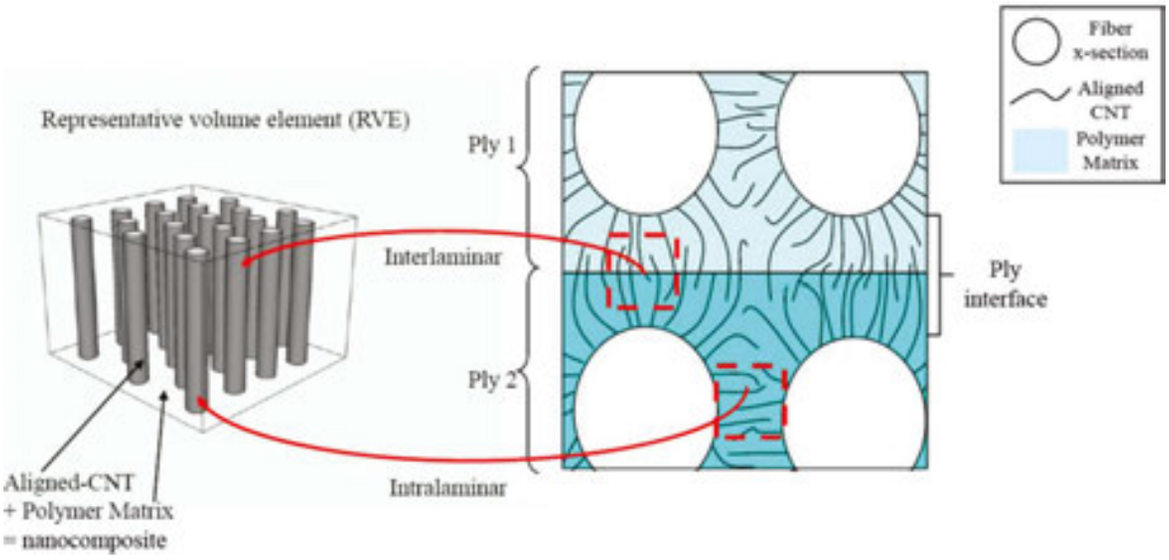

Figure 15. Schematic drawing of CNT reinforced composites, and aligned CNTs in a polymer as a representative volume element [65].

Bui et al. modified Duong's approach to investigate the thermal behavior of the SWNT-polystyrene (PS) composites at different volume fractions and at various temperature [67]. It was found that the thermal conductivity of SWNT-PS composites increased with the temperature rise. By validating with experimental data [68], the TBRs at both SWNT-PS and SWNT-SWNT interfaces were estimated by using the MC approach. The calculations at various temperature showed that the TBR between SWNT and PS increased with the rise of temperature. A TBR value of SWNT-SWNT was estimated to be 12.15×10^{-8} m^2K/W at 300K, which was higher than that between SWNT and PS (2.21×10^{-8} m^2K/W). Bui et al. also conducted the comparable study between graphene-polymer composites and SWNT-polymer composites [69]. The quantitative results showed that graphene nanosheets were more effective than SWNTs to enhance the thermal conduction in polymer composites.

5.2. Thermal conduction model for multi-phase aligned CNT composites

Recently, multiphase polymer composites, which contain more than one type of additive in the matrix, have attracted much attention [70,71]. The multiphase composites can combine the merits of all the components, inducing advanced multifunctional properties. Diverse multiphase polymer composites have been developed, such as CNT/nanoparticle/polymer composites [70,71], CNT/graphene/polymer composites [72,73], CNT/fiber/polymer composites [74,75] and CNT-stabilized polymer blends [76]. Since there is no effective approach to study thermal properties of CNT multiphase composites, Gong et al. [77] extended Duong's MC approach to investigate heat transfer phenomena in CNT multiphase composites. In Gong's model, a three-phase poly(ether ether ketone) (PEEK) composite containing SWNTs and tungsten disulfide (WS_2) nanoparticles was chosen as a case study, as shown in **Figure 16**(**a**) [78]. The TBRs at all interfaces (i.e. SWNT-PEEK, WS_2-PEEK and SWNT-SWNT) were taken into account in their model. The results showed that the thermal conductivity of multiphase

http://dx.doi.org/10.5772/62510

composites increased when the CNT concentration increased, and when the TBRs of CNT-PEEK and WS_2-PEEK interfaces decreased. The thermal conductivity of composites with CNTs aligned parallel to the heat flux was enhanced ~2.7 times relative to that of composites with randomly-dispersed CNTs.

The model could also quantitatively study the effect of the complex morphology and dispersion of SWNTs, (e.g., individual and bundled SWNTs, the number of SWNT bundles, and the number of SWNTs per bundle), on the thermal conductivity of multiphase composites. It was found that the TBR at the SWNT-SWNT interface played a significant role in the thermal conduction of the composite with SWNT bundles. As presented in **Figure 16**(**b**), the thermal conductivity of the three-phase composite decreased with the rise of SWNT-SWNT TBR. A critical SWNT-SWNT TBR was found to be 0.155×10^{-8} m^2K/W, which dominated the heat transfer mechanism in the three-phase composite. Proper treatment may be used to reduce the SWNT-SWNT TBR, such as the condensation of SWNT fibers, to enhance the thermal conductivity of multiphase composites with aligned SWNTs [78]. Besides the CNT multiphase composites, Gong et al. also modified the MC model to study the thermal conduction mechanisms in graphene composites [79] and CNT aerogels [80], as well as the multiphase biological systems containing CNTs [77,81,82], which indicated that the MC approach may be applicable for modeling heat transfer in diverse aligned CNT composite systems.

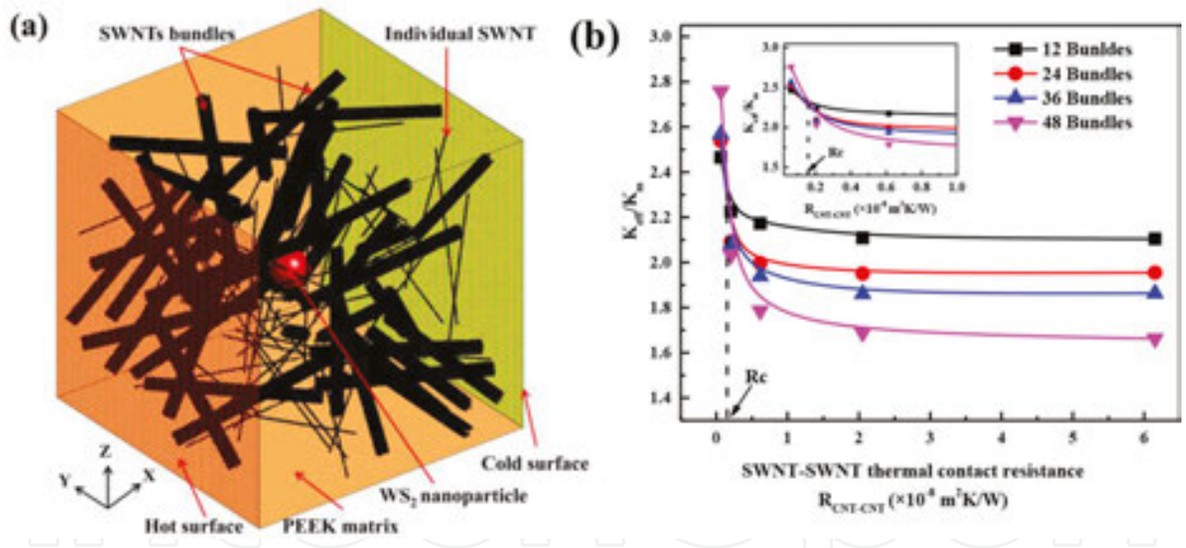

Figure 16. (a) Schematic plot of the computational model of the SWNT/WS_2/PEEK composites with SWNT bundles; (b) Effect of the SWNT-SWNT TBR on the thermal conductivity of the SWNT/WS_2/PEEK composites [78].

6. Conclusions and outlook

Both the CNT fibers and their polymer composites fabricated using the methods outlined in this article attain superior mechanical, electrical and thermal properties compared with CNT composites fabricated using the conventional methods. Their advanced properties make them

promising candidates for diverse applications, such as protective materials in airplanes and electrode materials in energy storage devices. For the diverse industrial applications of the aligned CNT composites, more studies should be carried out to fabricate the composites on a large scale and at low cost. New synthesis approaches can be developed to control the diameter of composite fibers and the size of composite films. To enhance their mechanical properties, cross linking should be created within CNT fibers through proper post-treatments. Chemical compositions and fabrication conditions require optimization for better polymer infiltration into the aligned CNT fibers, to achieve enhanced properties of the aligned CNT composites.

Author details

Hai M. Duong[1*], Feng Gong[1,2], Peng Liu[1] and Thang Q. Tran[1]

*Address all correspondence to: mepdhm@nus.edu.sg

1 Department of Mechanical Engineering, National University of Singapore, Singapore

2 School of Chemical, Biological and Materials Engineering, University of Oklahoma, USA

References

[1] Demczyk BG, Wang YM, Cumings J, Hetman M, Han W, Zettl A, et al. Direct mechanical measurement of the tensile strength and elastic modulus of multiwalled carbon nanotubes. Mater Sci Eng A. 2002;334(1–2):173-8.

[2] Pop E, Mann D, Wang Q, Goodson KE, Dai HJ. Thermal conductance of an individual single-wall carbon nanotube above room temperature. Nano Lett. 2006;6(1):96-100.

[3] Kim P, Shi L, Majumdar A, McEuen PL. Thermal transport measurements of individual multiwalled nanotubes. Phys Rev Lett. 2001;87(21):215502.

[4] Li QW, Li Y, Zhang XF, Chikkannanavar SB, Zhao YH, Dangelewicz AM, et al. Structure-dependent electrical properties of carbon nanotube fibers. Adv Mater. 2007;19(20):3358-63.

[5] Liu P, Lam A, Fan Z, Tran TQ, Duong HM. Advanced multifunctional properties of aligned carbon nanotube-epoxy thin film composites. Mater Design. 2015;87:600-5.

[6] Vennerberg D, Kessler MR. Anisotropic buckypaper through shear-induced mechanical alignment of carbon nanotubes in water. Carbon. 2014;80:433-9.

[7] Wardle BL, Saito DS, García EJ, Hart AJ, de Villoria RG, Verploegen EA. Fabrication and characterization of ultrahigh-volume- fraction aligned carbon nanotube–polymer composites. Adv Mater. 2008;20(14):2707-14.

[8] Roberto Guzmán de V, Namiko Y, Antonio M, Brian LW. Multi-physics damage sensing in nano-engineered structural composites. Nanotechnology. 2011;22(18): 185502.

[9] García EJ, Hart AJ, Wardle BL, Slocum AH. Fabrication and nanocompression testing of aligned carbon-nanotube–polymer nanocomposites. Adv Mater. 2007;19(16):2151-6.

[10] Jiang K, Li Q, Fan S. Nanotechnology: spinning continuous carbon nanotube yarns. Nature. 2002;419(6909):801.

[11] Vigolo B, Pénicaud A, Coulon C, Sauder C, Pailler R, Journet C, et al. Macroscopic fibers and ribbons of oriented carbon nanotubes. Science. 2000;290(5495):1331-4.

[12] Ericson LM, Fan H, Peng H, Davis VA, Zhou W, Sulpizio J, et al. Macroscopic, neat, single-walled carbon nanotube fibers. Science. 2004;305(5689):1447-50.

[13] Behabtu N, Young CC, Tsentalovich DE, Kleinerman O, Wang X, Ma AW, et al. Strong, light, multifunctional fibers of carbon nanotubes with ultrahigh conductivity. Science. 2013;339(6116):182-6.

[14] Zhang M, Atkinson KR, Baughman RH. Multifunctional carbon nanotube yarns by downsizing an ancient technology. Science. 2004;306(5700):1358-61.

[15] Zhang X, Li Q, Tu Y, Li Y, Coulter JY, Zheng L, et al. Strong carbon-nanotube fibers spun from long carbon-nanotube arrays. Small. 2007;3(2):244-8.

[16] Li Q, Zhang X, DePaula RF, Zheng L, Zhao Y, Stan L, et al. Sustained growth of ultralong carbon nanotube arrays for fiber spinning. Adv Mater- Deerfield Beach Then Weinheim. 2006;18(23):3160.

[17] Lepro X, Lima MD, Baughman RH. Spinnable carbon nanotube forests grown on thin, flexible metallic substrates. Carbon. 2010;48(12):3621-7.

[18] Zhu H, Xu C, Wu D, Wei B, Vajtai R, Ajayan P. Direct synthesis of long single-walled carbon nanotube strands. Science. 2002;296(5569):884-6.

[19] Li Y-L, Kinloch IA, Windle AH. Direct spinning of carbon nanotube fibers from chemical vapor deposition synthesis. Science. 2004;304(5668):276-8.

[20] Vilatela JJ, Windle AH. Yarn-like carbon nanotube fibers. Adv Mater. 2010;22(44): 4959-63.

[21] Motta M, Moisala A, Kinloch IA, Windle AH. High performance fibres from 'dog bone'carbon nanotubes. Adv Mater. 2007;19(21):3721-6.

[22] Wang J, Luo X, Wu T, Chen Y. High-strength carbon nanotube fibre-like ribbon with high ductility and high electrical conductivity. Nature communications. 2014;5. 3848. (DOI:10.1038/ncomms4848)

[23] Liu P, Tran TQ, Fan Z, Duong HM. Formation mechanisms and morphological effects on multi-properties of carbon nanotube fibers and their polyimide aerogel-coated composites. Compos Sci Technol. 2015;117:114-20.

[24] Tran TQ, Fan Z, Liu P, Myint SM, Duong HM. Super-strong and highly conductive carbon nanotube ribbons from post-treatment methods. Carbon. 2016;99:407-15.

[25] Koziol K, Vilatela J, Moisala A, Motta M, Cunniff P, Sennett M, et al. High-performance carbon nanotube fiber. Science. 2007;318(5858):1892-5.

[26] HowardáEbron V. Continuous carbon nanotube composite fibers: properties, potential applications, and problems. J Mater Chem. 2004;14(1):1-3.

[27] Kozlov ME, Capps RC, Sampson WM, Ebron VH, Ferraris JP, Baughman RH. Spinning solid and hollow polymer-free carbon nanotube fibers. Adv Mater. 2005;17(5):614-7.

[28] Kuznetsov AA, Fonseca AF, Baughman RH, Zakhidov AA. Structural model for dry-drawing of sheets and yarns from carbon nanotube forests. ACS Nano. 2011;5(2):985-93.

[29] Zhang Y, Zou G, Doorn SK, Htoon H, Stan L, Hawley ME, et al. Tailoring the morphology of carbon nanotube arrays: from spinnable forests to undulating foams. ACS Nano. 2009;3(8):2157-62.

[30] Huynh CP, Hawkins SC. Understanding the synthesis of directly spinnable carbon nanotube forests. Carbon. 2010;48(4):1105-15.

[31] Zhu C, Cheng C, He Y, Wang L, Wong T, Fung K, et al. A self-entanglement mechanism for continuous pulling of carbon nanotube yarns. Carbon. 2011;49(15):4996-5001.

[32] Liu K, Sun Y, Lin X, Zhou R, Wang J, Fan S, et al. Scratch-resistant, highly conductive, and high-strength carbon nanotube-based composite yarns. ACS Nano. 2010;4(10): 5827-34.

[33] Hill FA, Havel TF, Hart AJ, Livermore C. Enhancing the tensile properties of continuous millimeter-scale carbon nanotube fibers by densification. ACS Appl Mater Interf. 2013;5(15):7198-207.

[34] Natarajan B, Lachman N, Lam T, Jacobs D, Long C, Zhao M, et al. The evolution of carbon nanotube network structure in unidirectional nanocomposites resolved by quantitative electron tomography. ACS Nano. 2015;9(6):6050-8.

[35] Vigolo B, Poulin P, Lucas M, Launois P, Bernier P. Improved structure and properties of single-wall carbon nanotube spun fibers. Appl Phys Lett. 2002;81(7):1210-2.

[36] Miaudet P, Badaire S, Maugey M, Derré A, Pichot V, Launois P, et al. Hot-drawing of single and multiwall carbon nanotube fibers for high toughness and alignment. Nano Lett. 2005;5(11):2212-5.

[37] Sugano K, Kurata M, Kawada H. Evaluation of mechanical properties of untwisted carbon nanotube yarn for application to composite materials. Carbon. 2014;78:356-65.

[38] Tran CD, Humphries W, Smith SM, Huynh C, Lucas S. Improving the tensile strength of carbon nanotube spun yarns using a modified spinning process. Carbon. 2009;47(11): 2662-70.

[39] Miao M. Production, structure and properties of twistless carbon nanotube yarns with a high density sheath. Carbon. 2012;50(13):4973-83.

[40] Wang JN, Luo XG, Wu T, Chen Y. High-strength carbon nanotube fibre-like ribbon with high ductility and high electrical conductivity. Nature Commun. 2014;5.

[41] Liu K, Sun Y, Zhou R, Zhu H, Wang J, Liu L, et al. Carbon nanotube yarns with high tensile strength made by a twisting and shrinking method. Nanotechnology. 2010;21(4). 045708. (DOI: 10.1088/0957-4484/21/4/045708)

[42] Ounaies Z, Park C, Wise KE, Siochi EJ, Harrison JS. Electrical properties of single wall carbon nanotube reinforced polyimide composites. Compos Sci Technol. 2003;63(11): 1637-46.

[43] Jiang X, Bin Y, Matsuo M. Electrical and mechanical properties of polyimide–carbon nanotubes composites fabricated by in situ polymerization. Polymer. 2005;46(18): 7418-24.

[44] Zhu B-K, Xie S-H, Xu Z-K, Xu Y-Y. Preparation and properties of the polyimide/multi-walled carbon nanotubes (MWNTs) nanocomposites. Compos Sci Technol. 2006;66(3–4):548-54.

[45] So HH, Cho JW, Sahoo NG. Effect of carbon nanotubes on mechanical and electrical properties of polyimide/carbon nanotubes nanocomposites. Eur Polym J. 2007;43(9): 3750-6.

[46] Jiang Q, Wang X, Zhu Y, Hui D, Qiu Y. Mechanical, electrical and thermal properties of aligned carbon nanotube/polyimide composites. Compos Part B Eng. 2014;56:408-12.

[47] Sandler J, Shaffer MSP, Prasse T, Bauhofer W, Schulte K, Windle AH. Development of a dispersion process for carbon nanotubes in an epoxy matrix and the resulting electrical properties. Polymer. 1999;40(21):5967-71.

[48] Allaoui A, Bai S, Cheng HM, Bai JB. Mechanical and electrical properties of a MWNT/epoxy composite. Compos Sci Technol. 2002;62(15):1993-8.

[49] Moisala A, Li Q, Kinloch IA, Windle AH. Thermal and electrical conductivity of single- and multi-walled carbon nanotube-epoxy composites. Compos Sci Technol. 2006;66(10):1285-8.

[50] Liu W, Zhang X, Xu G, Bradford PD, Wang X, Zhao H, et al. Producing superior composites by winding carbon nanotubes onto a mandrel under a poly (vinyl alcohol) spray. Carbon. 2011;49(14):4786-91.

[51] Liu W, Zhao H, Inoue Y, Wang X, Bradford PD, Kim H, et al. Poly (vinyl alcohol) reinforced with large-diameter carbon nanotubes via spray winding. Compos Part A Appl Sci Manuf. 2012;43(4):587-92.

[52] Zhang L, Xu W, Luo XG, Wang JN. High performance carbon nanotube based composite film from layer-by-layer deposition. Carbon. 2015;90:215-21.

[53] Wang X, Yong Z, Li Q, Bradford PD, Liu W, Tucker DS, et al. Ultrastrong, stiff and multifunctional carbon nanotube composites. Mater Res Lett. 2013;1(1):19-25.

[54] Park JG, Cheng Q, Lu J, Bao J, Li S, Tian Y, et al. Thermal conductivity of MWCNT/epoxy composites: the effects of length, alignment and functionalization. Carbon. 2012;50(6):2083-90.

[55] Gong F, Bui K, Papavassiliou DV, Duong HM. Thermal transport phenomena and limitations in heterogeneous polymer composites containing carbon nanotubes and inorganic nanoparticles. Carbon. 2014;78(0):305-16.

[56] Han ZD, Fina A. Thermal conductivity of carbon nanotubes and their polymer nanocomposites: a review. Prog Polym Sci. 2011;36(7):914-44.

[57] Duong HM, Papavassiliou DV, Lee LL, Mullen KJ. Random walks in nanotube composites: improved algorithms and the role of thermal boundary resistance. Appl Phys Lett. 2005;87(1):013101.

[58] Einstein A. The electrodynamics of moving bodies. Ann Phys. 1905;17:891-921.

[59] Swartz ET, Pohl RO. Thermal-boundary resistance. Rev Mod Phys. 1989;61(3):605-68.

[60] Balandin AA. Thermal properties of graphene and nanostructured carbon materials. Nat Mater. 2011;10(8):569-81.

[61] Bui K, Papavassiliou DV. Numerical calculation of the effective thermal conductivity of nanocomposites. Num Heat Transfer Part A Appl. 2013;63(8):590-603.

[62] Duong HM, Papavassiliou DV, Mullen KJ, Wardle BL, Maruyama S. Calculated thermal properties of single-walled carbon nanotube suspensions. J Phys Chem C. 2008;112(50):19860-5.

[63] Duong HM, Papavassiliou DV, Mullen KJ, Wardle BL, Maruyama S. A numerical study on the effective thermal conductivity of biological fluids containing single-walled carbon nanotubes. Int J Heat Mass Transfer. 2009;52(23-24):5591-7.

[64] Duong HM, Papavassiliou DV, Mullen KJ, Maruyama S. Computational modeling of the thermal conductivity of single-walled carbon nanotube - polymer composites. Nanotechnology. 2008;19(6):065702.

[65] Duong HM, Yamamoto N, Papavassiliou DV, Maruyama S, Wardle BL. Inter-carbon nanotube contact in thermal transport of controlled-morphology polymer nanocomposites. Nanotechnology. 2009;20(15):155702.

[66] Duong HM, Yamamoto N, Bui K, Papavassiliou DV, Maruyama S, Wardle BL. Morphology effects on nonisotropic thermal conduction of aligned single-walled and multi-walled carbon nanotubes in polymer nanocomposites. J Phys Chem C. 2010;114(19): 8851-60.

[67] Bui K, Grady BP, Papavassiliou DV. Heat transfer in high volume fraction CNT nanocomposites: Effects of inter-nanotube thermal resistance. Chem Phys Lett. 2011;508(4-6):248-51.

[68] Peters JE, Papavassiliou DV, Grady BP. Unique thermal conductivity behavior of single-walled carbon nanotube–polystyrene composites. Macromolecules. 2008;41(20): 7274-7.

[69] Bui K, Duong HM, Striolo A, Papavassiliou DV. Effective heat transfer properties of graphene sheet nanocomposites and comparison to carbon nanotube nanocomposites. J Phys Chem C. 2011;115(10):3872-80.

[70] Naffakh M, Diez-Pascual AM, Gomez-Fatou MA. New hybrid nanocomposites containing carbon nanotubes, inorganic fullerene-like WS2 nanoparticles and poly(ether ether ketone) (PEEK). J Mater Chem. 2011;21(20):7425-33.

[71] Naffakh M, Diez-Pascual AM, Marco C, Ellis G. Morphology and thermal properties of novel poly(phenylene sulfide) hybrid nanocomposites based on single-walled carbon nanotubes and inorganic fullerene-like WS2 nanoparticles. J Mater Chem. 2012;22(4):1418-25.

[72] Yu AP, Ramesh P, Sun XB, Bekyarova E, Itkis ME, Haddon RC. Enhanced thermal conductivity in a hybrid graphite nanoplatelet - carbon nanotube filler for epoxy composites. Adv Mater (Weinheim, Germany). 2008;20(24):4740.

[73] Gupta TK, Singh BP, Mathur RB, Dhakate SR. Multi-walled carbon nanotube–graphene–polyaniline multiphase nanocomposite with superior electromagnetic shielding

[74] [77] Liao WH, Tien HW, Hsiao ST, Li SM, Wang YS, Huang YL, et al. Effects of multiwalled carbon nanotubes functionalization on the morphology and mechanical and thermal properties of carbon fiber/vinyl ester composites. ACS Appl Mater Interf. 2013;5(9):3975-82.

[75] Diez-Pascual AM, Ashrafi B, Naffakh M, Gonzalez-Dominguez JM, Johnston A, Simard B, et al. Influence of carbon nanotubes on the thermal, electrical and mechanical properties of poly(ether ether ketone)/glass fiber laminates. Carbon. 2011;49(8):2817-33.

[76] Cheng HKF, Basu T, Sahoo NG, Li L, Chan SH. Current advances in the carbon nanotube/thermotropic main-chain liquid crystalline polymer nanocomposites and their blends. Polymers. 2012;4(2):889-912.

[77] Gong F, Papavassiliou DV, Duong HM. Off-Lattice Monte Carlo simulation of heat transfer through carbon nanotube multiphase systems taking into account thermal boundary resistances. Num Heat Transfer Part A Appl. 2014;65(11):1023-43.

[78] [81] Gong F, Duong HM, Papavassiliou DV. Inter-carbon nanotube contact and thermal resistances in heat transport of three-phase composites. J Phys Chem C. 2015;119(14): 7614-20.

[79] Fan Z, Gong F, Nguyen ST, Duong HM. Advanced multifunctional graphene aerogel – Poly (methyl methacrylate) composites: experiments and modeling. Carbon. 2015;81(0):396-404.

[80] Gong F, Tam YS, Nguyen ST, Duong HM. Prediction of thermal resistances and heat conduction of carbon nanotube aerogels in various permeated gases. Chem Phys Lett. 2015;627:116-20.

[81] Gong F, Hongyan Z, Papavassiliou DV, Bui K, Lim C, Duong HM. Mesoscopic modeling of cancer photothermal therapy using single-walled carbon nanotubes and near infrared radiation: insights through an off-lattice Monte Carlo approach. Nanotechnology. 2014;25(20):205101.

[82] Fang Y, Lv Y, Gong F, Wu Z, Li X, Zhu H, et al. Interface tension-induced synthesis of monodispersed mesoporous carbon hemispheres. J Am Chem Soc. 2015;137(8):2808-11.